DEPLOYABLE ANTENNA REFLECTOR

By William B. Palmer

TRW, Defense and Space Systems Group

ABSTRACT

The first phase in the development of a solid surface, deployable, antenna reflector is outlined and discussed. The deployment concept is described in conjunction with illustrations and photos of the fabricated reflector models. Details and results of the thermal distortion analysis are presented. Results indicate that the discussed reflector concept is an effective approach in satisfying the requirements for large deployable antennas in the 6 GHz to 100 GHz frequency regime.

INTRODUCTION

Spacecraft communication at higher frequencies has led to a need for solid surface, parabolic antenna reflectors. These reflectors must have a high degree of contour accuracy, large diameter apertures and remain thermally stable in a space environment. Stowing larger reflectors inside the restricted envelope of a booster shroud requires developing a deployment concept without sacrificing surface contour accuracy.

An IR&D program was initiated by TRW, Defense and Space Systems Group, Redondo Beach, California in 1976. The first phase of the program was to develop a solid surface, deployable antenna reflector, for spacecraft operation, at frequencies up to 100 GHz. In this paper the progress delineated in developing a deployment concept conjoined with the utilization of the proper materials demonstrates the feasibility of providing a lightweight reflector that is thermally stable in space.

DEPLOYMENT CONCEPT

The deployment concept is illustrated in Figure 1. The center section is a one-piece honeycomb sandwich construction. All folding panels are rigid, honeycomb sandwich structure. The main panels hinge from a support ring under the center section. Two intermediate panels, between the main panels, are connected to the main panels with two or more hinges and to each other with two or more hinges. The hinges have adjustable stops to locate the panels accurately in the deployed position. Springs are used in the hinges to drive the panels to the deployed position. Adjacent inboard hinges of the main panels are interconnected with a compound universal coupling so that all panels deploy simultaneously. Deployment rate is controlled by either a damping device or a geared motor. The folded reflector is restrained by a pin puller, ordnance released, which is supported on one of the tie-down fittings. The tie-down fittings extend beyond the edge of the intermediate panels and are connected at a common joint on the reflector axis.

This concept has several advantages over other systems. For example, all panels are hinged together to insure close control of the parabolic contour.

Further, since the panels are interconnected with hinges, additional hinges or shear joints can be utilized on large reflectors to minimize the relative deflection at the panel joints. Also interconnection of the main panel hinges insures synchronized deployment, minimizing the chance of fouling or damaging panels. In addition insulation on the back of the panels can be used to reduce thermal distortion.

REFLECTOR SIZE AND CONFIGURATION

Although the antenna design and analysis was based on a 16-foot diameter reflector, the deployment concept is applicable for much larger reflectors. The design illustrated with 6 main panels hinged from the center section, is only one of many possible configurations. The number of main panels can be either decreased or increased to fit a particular set of requirements.

The ratios of deployed reflector diameters to stowed envelope dimensions is illustrated in Figure 2. It should be noted that to reduce the stowed envelope diameter requires more panels. The information in Figure 2 is based on preliminary layouts. Other configurations, using similar hinging techniques, may yield larger ratios of deployed/stowed dimensions but is a subject for future study. The graph illustrates the stowed envelope of 4, 6, 9, and 12 main panel configurations.

KINEMATICS

One of the main considerations in establishing the hinge lines was to provide clearance between the backs of the intermediate panels in the stowed position. The other consideration was to locate the hinge lines so that when the reflector was folded the panels would not be warped. Once the hinge lines were located then the shape of the panels was determined so that there would be no interference throughout deployment. A computer program was written to reduce the amount of descriptive geometry required. This program consists of establishing the coordinates of numerous points on the parabolic surface of the deployed reflector and then rotating these points to define the surface at any position during stowage. The paths of points in critical clearance areas were plotted in one degree increments of rotation near the deployed position. Clearance in the stowed position was established by connecting points along the edges of the panels to insure clearance with the contour of the adjacent panels.

REFLECTOR MATERIAL FOR 7-FOOT MODEL

The reflector was constructed of an aluminum honeycomb sandwich with graphite face sheets. The principal requirements were that the sandwich possess a low coefficient of expansion, be dimensionally stable and light as possible. GY70 graphite epoxy (50 ends per inch unidirectional with dacron fill and Narmco 5208 resin) was selected for the 7-foot diameter model. Each ply of the three ply face sheets was .003" thick and was oriented $0 \pm 60^\circ$. The aluminum core was 1.6 lb/ft^3 with ¼" cell size. A two stage layup was used to reduce panel weight. The face sheets were layed up and cured in an autoclave, then bonded to the core with a roller coating technique. The adhesive used for bonding the face sheets was HT424, a thixotropic paste, supplied by American Cyanamid. This material was selected because when applied with a roller it

forms a bead on the foil edges of the core for excellent bonding to the face sheet. The materials selected and the fabrication techniques used proved to be excellent selections because the completed panels revealed no distortion. The material properties as determined by testing are listed in Table 1.

DESIGN AND ANALYSIS OF 16-FOOT REFLECTOR

A 16-foot diameter reflector was chosen for a "paper" study. The study consisted of preliminary design, structural analysis, thermal distortion analysis and a weight estimate. The ½-inch thick sandwich construction for the reflector utilized three-ply graphite/epoxy face sheets, .009 inches thick, and an aluminum core with a ¼-inch cell size and density of 1.6 lb./ft^3. The support ring under the fixed center section was a rectangular tube cross-section 2 in. X 3 in. X .030 in. thick. The hinges interconnecting the panels were made of aluminum. The main panel inboard hinges which attach to the support ring were made of graphite epoxy composite. Because of weight considerations, no thermal control paint or insulation was used to reduce temperature gradients. Load factors of 12 g lateral and 10 g axial relative to the reflector axis were assumed for the structural analysis. Critical load paths were ascertained and components were sized accordingly.

THERMAL DISTORTION ANALYSIS

The thermal distortion model was a comprehensive model consisting of 1128 triangular plate elements representing the reflector. The support ring, hinges, and feed support struts were simulated by 232 members. Two TRW computer programs were used; the first to determine the deviation of the parabolic contour of each node and the second to determine the best-fit parabola through the nodes. From the Best-Fit Parabola program the ½-path length rms deviation, the focal length, and the bore-sight axis were ascertained.

Thermal distortion was computed for six different sets of conditions applicable for a synchronous orbiting spacecraft:

1. Front face fully illuminated, no insulation on back,
2. Front face ½ shaded, no insulation on back,
3. Front face ½ shaded, with insulation on back,
4. Front face 1/3 shaded, no insulation on back,
5. Front face ½ shaded, no insulation on back, $\alpha = + .3 \times 10^{-6}$ in/in/°F
6. Front face ½ shaded, no insulation on back, $\alpha = - .3 \times 10^{-6}$ in/in/°F
7. Front face ½ shaded, no insulation, inboard hinges of main panels graphite/epoxy composite,
8. Same as 7. except .25" thick core instead of .50"

The results are tabulated in Table 3. The first condition indicates that a symmetrically illuminated reflector has a minimal distortion. Condition 2 shows the effect of unsymmetrical illumination. Condition 3 indicates that adding insulation on the back does not reduce the distortion appreciably. Condition 4 demonstrates that the distortion is only slightly reduced with a small

shaded area. Conditions 5 and 6 show that a significant change in the coefficient of expansion of the graphite face sheets, $\alpha = \pm .3 \times 10^{-6}$ in/in/$^{\circ}$F, does not change the distortion drastically. On every other run $\alpha = - .15 \times 10^{-6}$ in/in/$^{\circ}$F. (Condition 7) all previous six conditions had aluminum hinges throughout. By changing only the inboard hinges of the main panels to a graphite/epoxy composite the distortion was greatly reduced. The core thickness was reduced from ½" to ¼" (Condition 8) with only a slight increase in distortion.

WEIGHT ESTIMATE

The preliminary weight estimate (Table 2) lists a total weight of 68.5 lbs for the 16-foot diameter reflector. The resultant weight per square foot of reflector surface is 0.299 lb/ft^2, including the weight of all components.

MODELS

A partial 7-foot diameter model (Figures 3-6), was designed and constructed of the same materials described for the 16-foot reflector. This model was used to verify that the materials and fabrication techniques would provide reflector panels with the required accuracy. It was also used to demonstrate the deployment concept.

An 11-inch demonstration model (Figures 7 and 8) was also constructed.

CONCLUDING REMARKS

The deployment concept was validated by deployment of the 7-foot diameter model. The accuracy of the surface contour for the panels of the 7-foot model demonstrated that the materials selected and the fabrication techniques were satisfactory for a high performance reflector. Analysis of the 16-foot diameter reflector showed that the distortion due to the worse case temperature distributions encountered in synchronous orbit was less than .002" rms and would be acceptable for frequencies as high as 60 GHz or more.

Future work will establish techniques for assembling, aligning and measuring surface accuracy of the reflector. Design verification tests should be run on flight antennas to demonstrate that the accuracy of the parabolic surface is not affected by launch, deployment or flight environments.
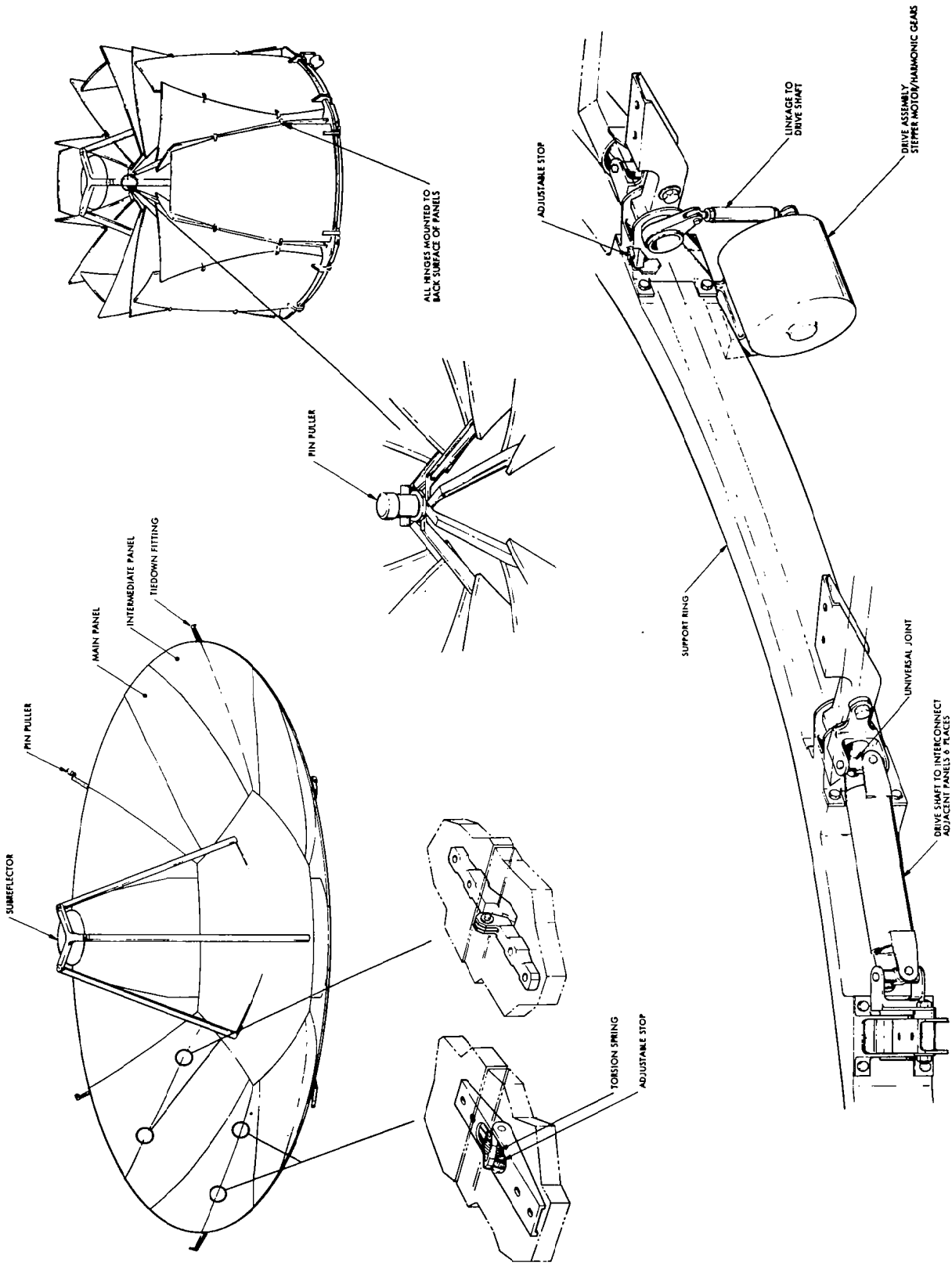
ALL HINGES MOUNTED TO
BACK SURFACE OF PANELS

PIN PULLER

LINKAGE TO
DRIVE SHAFT

DRIVE ASSEMBLY
STEPPER MOTOR/HARMONIC GEARS

ADJUSTABLE STOP

MAIN PANEL

INTERMEDIATE PANEL

TIEDOWN FITTING

PIN PULLER

SUBREFLECTOR

SUPPORT RING

UNIVERSAL JOINT

DRIVE SHAFT TO INTERCONNECT
ADJACENT PANELS 6 PLACES

TORSION SPRING

ADJUSTABLE STOP

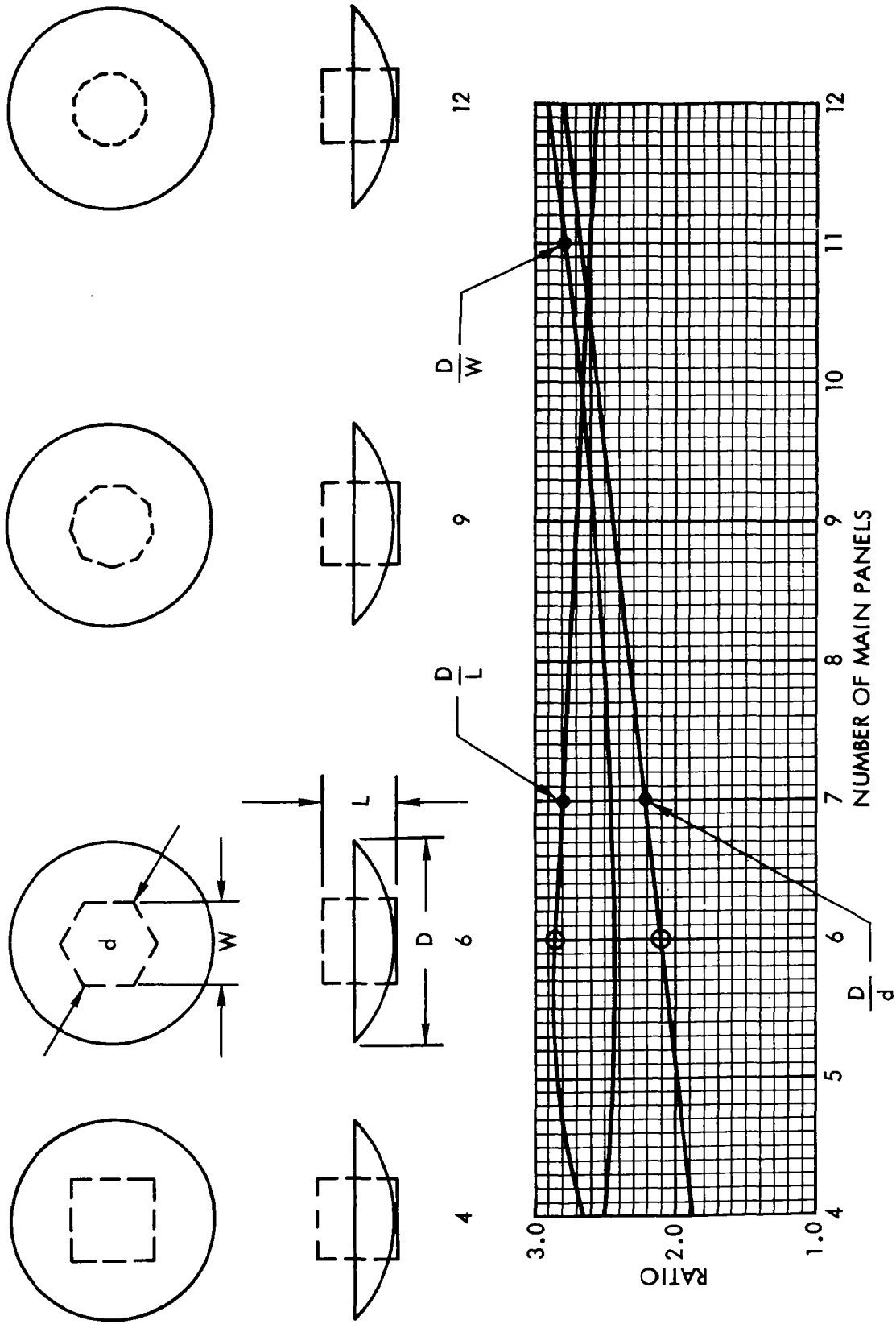Figure 1   Solid Deployable Reflector

Figure 2   Reflector Configurations and Ratios Of Diameter
To Stowed Envelope Dimensions

228

about 2.5 cm (1 inch) of 0.508 mm (0.020 inch), or about 8 cm (3 inch) of 0.794 mm (1/32-inch) tubing should be helpful for gust filtering without introducing undesirable delays, even if the capacitor volume is small.

FLOW FIELD EFFECTS ON TOTAL ENERGY SENSORS

Obtaining the pressure coefficient for good compensation is best achieved if the sensor can be located in the freestream, unaffected by attitude changes of the aircraft. It is not necessary that the local pressure be the same absolute value as the freestream; it is only necessary that the static pressure, relative to freestream, not vary as the aircraft attitude changes. Because of this, a desirable sensor location must take into consideration local flow field changes during maneuvers. There are several aspects of flow fields which may be important:

1. Boundary layer growth along the body

2. Flow angularities caused by the windshield and the wing body
        intersection

3. Downwash caused by lifting surfaces deflecting the flow

4. Movable control surfaces which may propagate pressure influences
        upstream

5. Induced velocities above wing or fuselage

The boundary layer consideration is largely relevant if probes are located on the aft portion of the fuselage. Flows tend to parallel fuselage surfaces aft of the wing, so that a location roughly mid-way between the wing trailing edge and the tail offers relatively constant flow conditions for total energy sensors, provided that the sensor is located far enough from the body to avoid the boundary layer at all angles of attack or yaw. For aft fuselage mounting on the upper side, the sensor element should be located about 7 inches above the surface to insure avoidance of boundary layer fluctuations as attitude changes.

Sensors have been located successfully on the noses of sailplanes; however, for this location there often are significant flow angularities as the flow streamlines are diverted around the body. Canopy bumps may cause local effects which would be undesirable, for example, and when positioning at the proper sweep angle, it should be recognized that streamlines parallel the surface at the surface.

High performance sailplanes usually achieve some laminar flow on the nose portion of the fuselage; a performance penalty may result with a probe in the laminar region which triggers an early transition from laminar to turbulent flow. This is not a problem for training sailplanes or others which do not depend on laminar flow for performance. Judgement must be

used in determining the proper sensor sweep angle on a curving surface, and experimenting with flight tests may be necessary.

The vertical fin location usually offers near freestream conditions, provided the probe is positioned so that the fin, rudder, stabilizer and elevator (especially for Tee Tail configurations) are taken into account.

The principal downwash in the flow field at the fin location is caused by the wing deflecting the air to produce lift. A series of calculations have been made to cover the range of effects for typical sailplanes during cruise and climb conditions. The downwash flow angle is a function of the lift coefficient being achieved at a given time. Reference 16 provides a thorough discussion of the mechanisms affecting the downwash as well as analytical methods for use in calculations. Based on these techniques, and the dimensions for short coupled sailplanes like the 1-26, the down-wash angle at the fin tip in degrees is about three times the lift coefficient, C_L . In the cruise condition, the lift coefficient for the 1-26 is about 0.5, making the downwash angle only 1.5 degrees. In the climb condition, the lift coefficient is about 1, making the downwash about 3^0. For high performance sailplanes having longer wings and fuselages, the downwash values decrease to about half those for a 1-26; that is, the range of downwash angles at the fin may be about 1.2 to 1.8 times C_L degrees. The range of lift coefficients may be somewhat greater due to flaps; however, the total downwash variation for high performance sailplanes may still be less than 3^0.

For a fin installation, the sensor should be positioned at least 5 to 10 times the maximum fin thickness ahead of the leading edge (ref. 17). Severe rudder deflections may cause significant lateral flow inclinations; however, the insensitivities of the simple probes described herein are a real advantage. Horizontal tail movements affect the downwash flow field to some extent. When attitude changes are being made, transients may be noticed; however, the effects can be minimized by smooth movements of the control surfaces. Sailplanes that are well balanced will not have very large tail lift coefficients, and therefore small downwash effects.

In summary, a sensor location insensitive to changes in attitude is necessary for operation over a broad range of locations. Aft fuselage and vertical fin locations can be suitable for the probes discussed. Nose installations may be acceptable for low performance sailplanes; however, they must be positioned carefully.

230

CONCLUDING REMARKS

Experimental pressure coefficients suitable for total energy compensation have been obtained using principles of laminar flow around a small inclined cylinder. To obtain the correct flow relationships, the sensor orifice should be located carefully with respect to the end of a 3-dimensional cylinder; several options for providing the proper relationships have been extended by the current study of probes made of bent-up tubing. Total energy-pressure relationships have been reviewed to explain the principles involved and further explanations of 3-dimensional effects have been presented.

In general, it has been shown that probe sensors with lengths as short as 7 times the outside diameter of the tubing used can be made to work with certain orifice locations. On the other hand, data have shown that sensitivities to manufacturing tolerance and flow incidence angles are reduced when sensor lengths of 11 diameters or greater are used.

Comparative results from a number of experimenters have verified the principles and findings previously presented. The most significant of these probe dimensions are the sensor hole location geometry and the best angle of sweep for compensation that is insensitive to range of angles of incidence.

Damping restrictors are useful to filter gusts and may be simply made by installing a small section of capillary tubing in or near the total energy probe, in series with an appropriate capacitor volume.

Flow field effects around aircraft can affect the compensation of total energy sensors and must be considered. Among the effects are the boundary layer growth, flow angularities, downwash caused by lifting surfaces and movable control surfaces which may propagate pressure influences. The significance of these effects and ways of accounting for them are discussed.

REFERENCES

1. Nicks, Oran W.: A Simple Total Energy Sensor. NASA TMX-73928, March 1976. (Also presented at XV Congress of OSTIV, Rayskala, Finland, June 1976.)

2. Nicks, Oran W.: A Simple Total Energy Sensor. Soaring, Volume 40, No. 9, Sept. 1976.

3. Nicks, Oran W.: How to Make a Total Energy Sensor. Soaring, Vol. 41, No. 3, March 1977.

4. U. S. Patent Office, U. S. Patent No. 4,061,028. Aircraft Total Energy Sensor - Oran W. Nicks, Dec. 6, 1977.

5. Thom, A.: The Flow Past Circular Cylinders at Low Speeds. Proceedings of the Royal Society of London, Series A., Vol. CXLI. Printed for the Royal Society and sold by Harrison and Sons, Ltd., St. Martins Lane, Sept. 1933.

6. Thom, A.: An Investigation of Fluid Flow in Two Dimensions. Reports and Memoranda No. 1194 (AE356). Printed and Published by His Majesty's Stationary Office, London, Nov. 1928.

7. Goldstein, S.: Modern Developments in Fluid Dynamics. Vol. I, Oxford at the Clarendon Press, 1938.

8. Bursnall, William J., and Loftin, Laurence K., Jr.: Experimental Investigation of the Pressure Distribution About a Yawed Circular Cylinder in the Critical Reynolds Number Range. NACA TN 2463, Sept. 1951.

9. Wells, Bill: Calibrating Total Energy Tubes. Soaring, Vol. 41, No. 11, Nov. 1977.

10. Westerboer, Ingo: Die Neue Nicks-Duse: Ein ganz heiber Tip von der OSTIV-Tagung in Finnland. aerokurier, Vol. 9, Sept. 1976.

11. Shaw, Charles: T. E. Sensor, 1-26 Association Newsletter, Jan. 1977.

12. Irving, Frank: A New Total Energy Head. Sailplane and Gliding, Feb.-March 1978.

13. Johnson, Dick: Variometer Time Constants - Soaring Mail - Soaring Vol. 41, No. 6, June 1977.

14. Foster, K., and Parker, G. A.: Fluidics Components and Circuits. Wiley Interscience, A Division of John Wiley and Sons, Ltd., London, New York, Sydney, Toronto.